Sway and Roll Hydrodynamics of Twin Rectangular Cylinders

Jonathan D. Elkin and Ronald W. Yeung
Department of Mechanical Engineering
University of California at Berkeley, Berkeley, CA 94720-1740, USA
E-mail: *jelkin_99@yahoo.com* & *rwyeung@berkeley.edu*

1 Introduction and Background

Resonance of the fluid in the gap between two floating bodies is known to greatly affect their hydrodynamic properties. The added-mass coefficients of twin bodies will, for certain ranges of the frequency domain, attain large positive and then negative values. Nearby, the damping coefficient will vanish and then attain a large value (or vice versa). In contrast, these same coefficients of a *single* floating body are generally less "volatile" across the frequency range, exhibiting at most one local (and global) maximum.

This interesting behavior was first studied by Wang and Wahab (1971) for the case of twin, semi-submerged, circular, horizontal cylinders in synchronous heave. They found that, for certain frequencies of oscillation, a standing wave existed in the gap between the bodies, resulting in the notable hydrodynamic behavior mentioned above. The fundamental frequency and harmonics for which this resonance occurred could, in general, be predicted by an equation for symmetric standing waves in the gap between the bodies, with wave forms having zero slopes at the walls. They also observed a so-called "zeroth-order," or Helmholtz, resonance, which is characterized by an almost piston-like movement of the fluid in the gap, in which the free surface remains essentially horizontal. Similar three-dimensional behavior of this type was also observed for an array of cylinders by a number of workers (e.g., Yeung and Sphaier, 1989).

The renewed interest in catamaran-hull designs in recent years, including applications in fast ferries and naval craft, has led to further studies of these twin-body problems. Seah (2006) and Yeung and Seah (2007) recently studied the case of twin rectangular bodies oscillating in heave. They examined carefully the shape of the free surface in the moonpool near these resonances. They also noted that the frequencies at which heave damping vanishes do not necessarily correspond to those of maximum moonpool motion, but the vanishing of damping is an effective way of "marking" these resonance points. The present work considers the same geometry, but for the case of sway and roll motion.

We note that shapes can be generated for a *single* body to have zero damping at specfic frequencies, as in Kyozuka and Yoshida (1981). Since radiation damping of a body is directly related to the wave-exciting force (Wehausen, 1971), such zero-damping frequencies, if coincident with the dynamical resonant frequency of the floating body, will yield body motion with an amplitude proportional to the inverse of the square root of the damping. The motion will then be unbounded, per linear theory.

Another phenomenon related to such free-surface problems is the occurrence of trapped modes, which correspond to the existence of nontrivial homogeneous solutions for certain special shapes and at certain frequencies (McIver, 1996). These are wave-free solutions, which correspond also to zero damping, but are not related to the vanishing of damping near resonance discussed above.

2 Solution Representations

The problem is solved semi-analytically using the method of matched eigenfunction expansions — the same method used by Seah (2006) and Yeung and Seah (2007) for the twin-body heave case, and before that for various single-body cases by Fotsch (1997), Ra (1997), and Yeung (1981). It has the benefits of being accurate, free from irregular frequencies, and fairly rapidly convergent.

Within the framework of the usual linearized, inviscid-fluid, small-motion hydrodynamic theory, the radiation potentials are sought in *each* of the subdomains (Fig. 1), subject to body boundary conditions

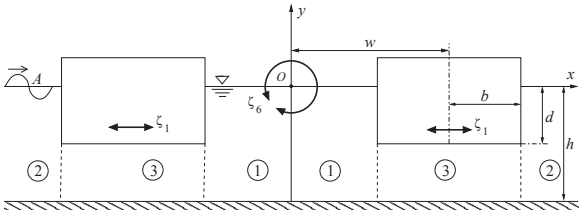

Figure 1: Geometry of cylinders and fluid subdomains.

on the cylinders, which are motion-specific.

The problem in each region is solved in terms of the solutions for each neighboring region, as if they were known *a priori*, but subject to flux and fluid-pressure continuity along the vertical interfaces. This results in a set of simultaneous, linear equations for the coefficients of the modal functions in each subdomain. Once the radiation problem has been solved, the wave-exciting force, via the use of Haskind's relation, and the response amplitude operator can also be determined with relatively little additional work.

We write the radiation potential as:

$$\Phi_j(x,y,t) = Re[-i\sigma\zeta_j\varphi_j(x,y)\mathrm{e}^{-i\sigma t}]\,, \qquad (1)$$

where σ is the angular frequency of oscillation and ζ_j is the amplitude of sway ($j=1$) or roll ($j=6$) motion. The spatial potential φ_j, with the subscript j omitted for convenience henceforth, is understood to be mode-dependent and is defined piecewise across the fluid domain as

$$\varphi\,(x,y) = \begin{cases} \varphi^q & q = e1, e2, \text{for Region 1, 2;} \\ \varphi^i & \text{for Region 3.} \end{cases}$$

Because of the antisymmetry of the problem about $x=0$, we require $\varphi(0,y)=0$ and need to consider only the right side of the fluid domain, $x \geq 0$.

The kinematic boundary conditions on the body are well known. In the present notation, we write

$$\begin{array}{ll} \varphi_x(w \mp b, y) = f^q & \text{for Region 1, 2;} \\ \varphi_y(x,-d) = f^i & \text{for Region 3} \end{array} \qquad (2)$$

with $f^{e1} = f^{e2} = 1$ and $f^i = 0$ for sway motion ($j=1$), and $f^{e1} = f^{e2} = -y$ and $f^i = x$ for roll motion ($j=6$) about the *coordinate origin O*.

Throughout the fluid, φ must satisfy the Laplace equation. In Regions 1 and 2, the usual time-harmonic linearized free-surface and no leak bottom conditions are imposed, with an outgoing (and bounded amplitude) wave condition in Region 2. Continuity of fluid pressure and flux at the vertical interface requires

$$\begin{array}{ll} \varphi^i = \varphi^{e1}\,,\ \varphi^i_x = \varphi^{e1}_x\,, & \text{at } x = w-b, \\ \varphi^i = \varphi^{e2}\,,\ \varphi^i_x = \varphi^{e2}_x\,, & \text{at } x = w+b. \end{array} \qquad (3)$$

2.1 "Exterior" Solutions for $q = e1, e2$

In these external regions, the general solutions can be obtained by separation of variables. Those in Region 2 are like a 2-D wavemaker, whereas those in Region 1 correspond to antisymmetric versions of the solution found by Seah (2006). Both can be written in the form

$$\varphi^q(x,y) = \sum_{k=0}^{\infty} B^q_k \Lambda^q_k(x) Y^e_k(y), \quad q = e1, e2 \qquad (4)$$

with the B^q_k being coefficients to be determined. Here,

$$\Lambda^{e1}_k\,(x) = \begin{cases} \sin m_0 x / \sin m_0(w-b), & k=0 \\ \sinh m_k x / \sinh m_k(w-b), & k \geq 1 \end{cases}$$

$$\Lambda^{e2}_k\,(x) = \begin{cases} \mathrm{e}^{im_0[x-(w+b)]}, & k=0 \\ \mathrm{e}^{-m_k[x-(w+b)]}, & k \geq 1 \end{cases}$$

$$Y^e_k\,(y) = \begin{cases} \cosh m_0(y+h)/\sqrt{N_0}, & k=0 \\ \cos m_k(y+h)/\sqrt{N_k}, & k \geq 1 \end{cases}$$

The eigenvalues m_k ($k = 0, 1, 2, \ldots$) given by the imaginary ($k=0$) and real ($k \geq 1$) roots of $\nu h = -m_k h \tan m_k h$, $\nu \equiv \sigma^2/g$, are well known. The vertical functions $\{Y^e_k\}$, with the scale factor N_k, form an orthonormal set in the interval $y = [-h, 0]$.

2.2 "Interior" Solution

The possibly inhomogeneous body boundary condition [for $j=6$ in (2)] leads us to write the interior solution φ^i as the sum of a homogeneous solution φ^i_h and an appropriate particular solution φ^i_p. For sway motion ($j=1$), $\varphi^i_p = 0$. For roll motion ($j=6$), a particular solution is given by (Ra, 1997):

$$\varphi^i_p = \left[x\,(y+h)^2 - x^3/3\right]/(2(h-d)).$$

The homogeneous solution is

$$\varphi^i_h\,(x,y) = \sum_{n=0}^{\infty} \left[C_{1n}X_{1n}(x) + C_{2n}X_{2n}(x)\right] Y^i_n\,(y)\,,$$

where X_{2n} and X_{1n} correspond to symmetric and antisymmetric terms about the centerline of the *cylinder* ($x=w$), respectively, and

$$Y^i_n(y) = \frac{\cos\gamma_n(y+h)}{\sqrt{N^i_n}}, \quad \gamma_n = \frac{n\pi}{h-d}, \quad n = 0, 1, \ldots$$

with $N^i_0 = 1, N^i_n = \frac{1}{2}$. The set $\left\{Y^i_n\right\}$ is orthonormal in the interval $y = [-h, -d]$. C_{1n} and C_{2n} are coefficients to be determined.

2.3 Coupling of Solutions

The form of the solutions in each region is now known; what remains is to determine the coefficients B^{e1}_k and B^{e2}_k for $k = 0, 1, 2, \ldots$, and C_{1n} and C_{2n} for $n = 0, 1, 2, \ldots$. This is accomplished by applying the interfacial "matching" conditions to the solutions found thus far. Using the orthonormal properties of the $\{Y^e_k\}$ and $\left\{Y^i_n\right\}$ sets, we obtain a set of explicit equations for B^q_k in terms of C_{1n} and C_{2n}, and for $C_{2n} \mp C_{1n}$ in terms of B^q_k:

$$B^q_k = \frac{1}{h\left(\Lambda^q_k\right)'}\left[\int_{-h}^{-d} \varphi^i_x Y^e_k \mathrm{d}y + \int_{-d}^{0} f^q\, Y^e_k \mathrm{d}y\right] \qquad (5)$$

$$C_{2n} \mp C_{1n} = \left\langle \varphi^q, Y_n^i \right\rangle_i - \left\langle \varphi_p^i, Y_n^i \right\rangle_i , \qquad (6)$$

both of which are to be evaluated at $x = w - b$ for $q = e1$ and at $x = w + b$ for $q = e2$. Recall that in (5), φ_h^i is (the sum of) a series involving C_{1n} and C_{2n}. Conversely, in (6), φ^q is a series involving B_k^q.

Substitution of (5) into (6) gives

$$\begin{aligned} C_{2n} \mp C_{1n} &- \sum_{j=0}^{\infty}\sum_{k=0}^{\infty} \frac{\Lambda_k^q}{\left(\Lambda_k^q\right)'} \\ &\times \frac{1}{h\,(h-d)} \left(C_{1j}X'_{1j} + C_{2j}X'_{2j}\right) S_{kj}S_{kn} \\ &= \sum_{k=0}^{\infty} \frac{\Lambda_k^q}{\left(\Lambda_k^q\right)'} \cdot \frac{S_{kn}}{h\,(h-d)} \left[\int_{-h}^{-d} \varphi_{p,x}^i Y_k^e \mathrm{d}y \right. \\ &\left. + \int_{-d}^{0} f^q Y_k^e \mathrm{d}y \right] - \left\langle \varphi_p^i, Y_n^i \right\rangle_i , \quad n = 1, 2, \ldots . \qquad (7) \end{aligned}$$

where S_{kn} is given in Seah (2006). Here, the only unknowns are C_{1n} and C_{2n}, which are all located on the left-hand side; the right-hand side can be evaluated explicitly. By truncating the infinite sums after N terms, (7) will yield a set of $2N$ simultaneous linear equations in these unknowns. Once these are solved, (5) can be used to find B_k^q; hence, φ is known everywhere.

3 Representative Results

The solution of this antisymmetric, twin-body problem depends on the frequency parameter νb and three other parameters that are geometric: w/b [or $(w - b)/b$], d/b, and h/d. Only some representative and interesting results will be covered in this paper.

The variation of the sway damping ($\overline{\lambda_{11}}$) and added-mass ($\overline{\mu_{11}}$) coefficients, normalized by $\rho\sigma b^2$ and ρb^2, is compared with a baseline heave-motion solution in Figs. 2–3 for $d/b = 1, (w - b)/b = 4$, and $h/d = 20$. As expected, the Helmholtz mode is absent for sway (and roll), but there are similar rapid variations around the resonance points for all three modes of motion. As in the heave case, there exist zero damping points next to spiky damping values and the zero crossings of the added mass coincide with the peaks of the damping. However, the first zero-damping point of sway occurs to the left of the damping spike, whereas the corresponding point for heave and roll is to the right of the spike.

Figs. 4–5 show the sway added mass and damping alongside the roll added inertia and damping (normalized similarly) versus $\nu(w - b)/(\pi/2)$, a gap-based frequency. The qualitative features of the results for sway and roll are similar, with the vertical scale depending on the way normalization is carried out. In both cases, the zero damping points match closely with the equation:

$$\frac{\nu(w-b)}{\pi/2} = \frac{2(w-b)}{\lambda/2} = n, \quad n = 1, 3, 5, \ldots , \qquad (8)$$

the first equality holding for deep water. This states that the full moonpool width is an odd multiplier of one-half of the wavelength λ — a standing-wave condition. An appropriate parameter that gauges the occurence of resonance with the water-depth effects embedded is therefore $m_o(w - b)$, subject to sufficiently large d/b. The narrow-bandedness of the higher-order resonances implies that they are not easily detectable physically, as viscous effects will come into play because of flow separation at the sharp corners (Yeung, 2002). Fig. 6 shows the effects on the sway added mass and damping of widening the moonpool gap significantly. In this figure, we superpose the results of two (non-interacting) single rectangular cylinders of the same dimensions as one demihull. Note the disappearance of the negativity of the added mass in the lower-order resonances, yet the damping points retain their vanishing values based on Eq. (8). Both coefficients maintain their wildly oscillatory behavior.

Fig. 7 is an assessment of the convergence characteristics of the series. The vertical axis represents the *relative* error in μ_{11} resulting from using N terms in the expansion, rather than using $N = 120$ terms (normalized by the 120-term value). A relative accuracy of 10^{-3} is easily attainable. Interestingly, even values of N are more accurate than nearby odd values!

Finally, in Fig. 8 we show one case of results of the roll response ampitude and phase angle of the twin cylinder with $\overline{BG} = 0$. These were obtained by using the roll radiation solution and the Haskind relation. Besides the usual "dynamic resonance," there are now also peaks in the response associated with the *hydrodynamic* resonance. These and other results will be discussed in the Workshop.

References

[1] Fotsch, A. R. (1997). Graduate Student Paper, SNAME Northern Calif. Section, April 10, 31 pp.

[2] Kyozuka, Y. and Yoshida, K. (1981). *Appl. Ocean Res.*, **3**(4), 183–194.

[3] McIver, M. (1996). *J. Fluid Mech.*, **315**, 257–266.

[4] Ra, B. (1997). M.S. Thesis, Univ. of California at Berkeley, August, 61 pp.

[5] Seah, R. K. M. (2006). Graduate Student Paper, SNAME Northern Calif. Section, Feb. 15, 20 pp.

[6] Wang, S. and Wahab, E. (1971) *J. Ship Research*, **15**(1), 33–48.

[7] Wehausen, J. V. (1971). *Ann. Rev. Fl. Mech.*, **3**, 237–268.

[8] Yeung, R. W. (1981). *Appl. Ocean Res.*, **3**, 119–133.

[9] Yeung, R. W. and Sphaier, S. H. (1989). *J. Engrg. Math.* **23**(2), 95-117.

[10] Yeung, R. W. (2002). *Proc., 12th Int'l Offshore and Polar Eng. Conf.*, Kitakyushu, Japan, **2**, 1–11.

[11] Yeung, R. W. and Seah, R. K. M. (2007). *J. Engrg. Math.* **41**(1) (In press).

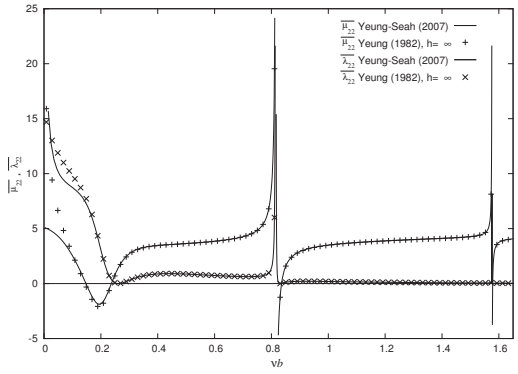

Figure 2: $\overline{\mu_{22}}$ and $\overline{\lambda_{22}}$ vs. frequency νb for heave: $d/b = 1$, $\frac{w-b}{b} = 4$, $h/d = 20$ (Yeung & Seah, 2007).

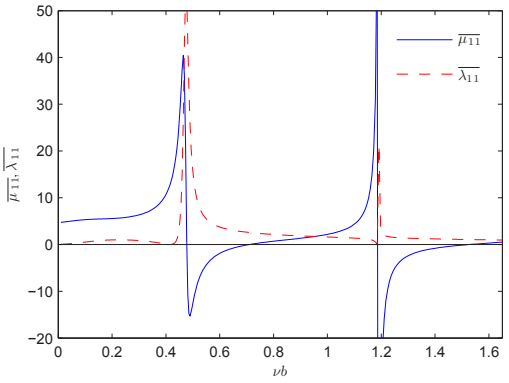

Figure 3: $\overline{\mu_{11}}$ and $\overline{\lambda_{11}}$ vs. frequency νb for sway: $d/b = 1$, $(w-b)/b = 4$, $h/d = 20$ (present theory).

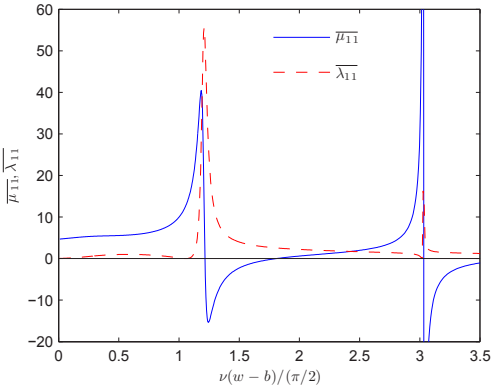

Figure 4: $\overline{\mu_{11}}$ and $\overline{\lambda_{11}}$ vs. frequency $\nu(w-b)/(\pi/2)$ with $d/b = 1$, $(w-b)/b = 4$, $h/d = 20$.

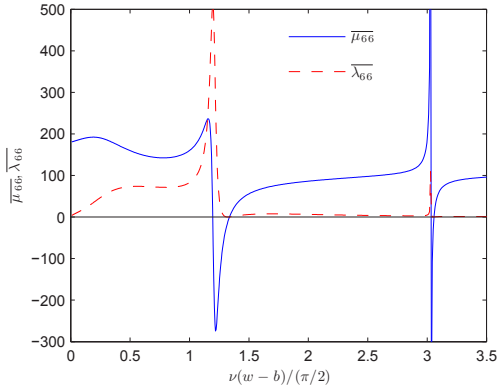

Figure 5: $\overline{\mu_{66}}$ and $\overline{\lambda_{66}}$ vs. frequency $\nu(w-b)/(\pi/2)$ with $d/b = 1$, $(w-b)/b = 4$, $h/d = 20$.

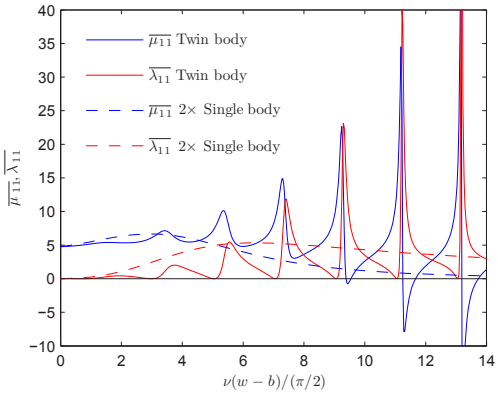

Figure 6: Sway $\overline{\mu_{11}}$ and $\overline{\lambda_{11}}$ for a very wide gap with $(w-b)/b = 40$, $d/b = 1$, $h/d = 20$.

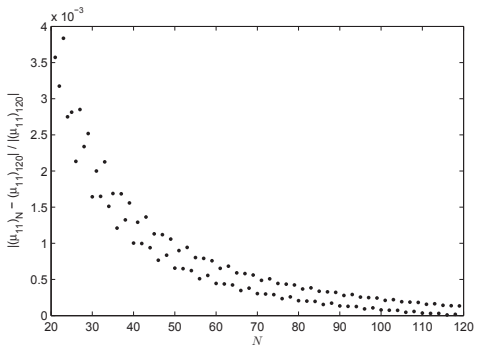

Figure 7: Modulus of error of $\overline{\mu_{11}}$ computed with N terms, relative to $\overline{\mu_{11}}$ computed with 120 terms, for $\nu b = 0.9$, $d/b = 0.9$, $(w-b)/b = 1.1$, $h/d = 5$.

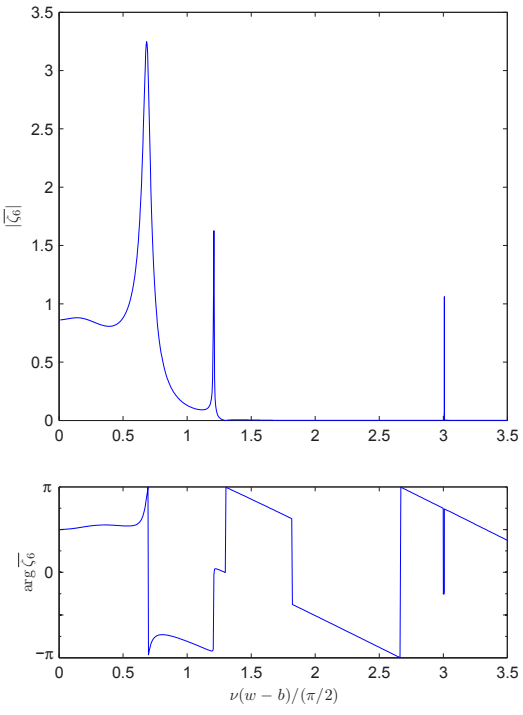

Figure 8: Roll response amplitude (above) and phase angle (below) vs. gap-frequency for $d/b = 2$, $(w-b)/b = 4$, $h/d = 20$.